

ESO observing programme: Core And Filament Formation and Evolution In Natal Environments (CAFFEINE)

Abstract

We release advanced imaging data products in FITS format for the ESO project IDs E-1102.C-0745A-2018 and 106.21MS, which were obtained with the ArTéMiS camera at the APEX telescope, located at 5100 m in Llano de Chajnantor, in the Atacama desert, during 8 epochs from 2018 to 2022 (for details about ArTéMiS, see André et al. 2016 and references therein). The observations cover the 350 μm and 450 μm atmospheric bands in parallel, and have a resolution of 8'' and 10'' (half-power beam width), respectively.

The released data products are comprised of 350 μm and 450 μm intensity maps and multi-resolution column density maps, based on these data. The 48 imaged fields cover a total area of more than $\sim 2.5 \text{ deg}^2$, focused on the dense ($A_V > 10$) parts of molecular clouds within about 3 kpc from the Sun. The intensity maps have been combined with data from the *Herschel*/SPIRE instrument, taken at similar wavelengths, to recover large scale emission that cannot be detected from the ground with ArTéMiS. The column density maps have been derived by including additional *Herschel* data at 160 μm and 250 μm and fitting the observed spectra energy distributions between 160 μm and 450 μm on a pixel-to-pixel basis. They have been created using the multi-resolution decomposition technique described in Schuller et al. 2021 and Appendix A of Palmeirim et al. 2013, and have a resolution ranging from $\sim 8''$ in their denser inner parts ($A_V > 40$) to 18.2'' in the lower-density outer parts ($A_V < 40$). They are based on the same dust opacity assumptions as the 18.2''-resolution column density maps of the *Herschel* Gould Belt survey (cf. André et al. 2010, A&A, and Roy et al. 2014, A&A).

Overview of Observations

The imaging data products are based on 961 on-the-fly maps taken with ArTéMiS, which have been reduced, calibrated, and combined into 48 separate fields. For each field, we provide two ArTéMiS/SPIRE intensity maps at wavelengths of 350 μm and 450 μm , along with the corresponding ArTéMiS weight maps, and a multi resolution column density map. The locations of the observed fields in the Galactic Plane are shown in Fig. 1.

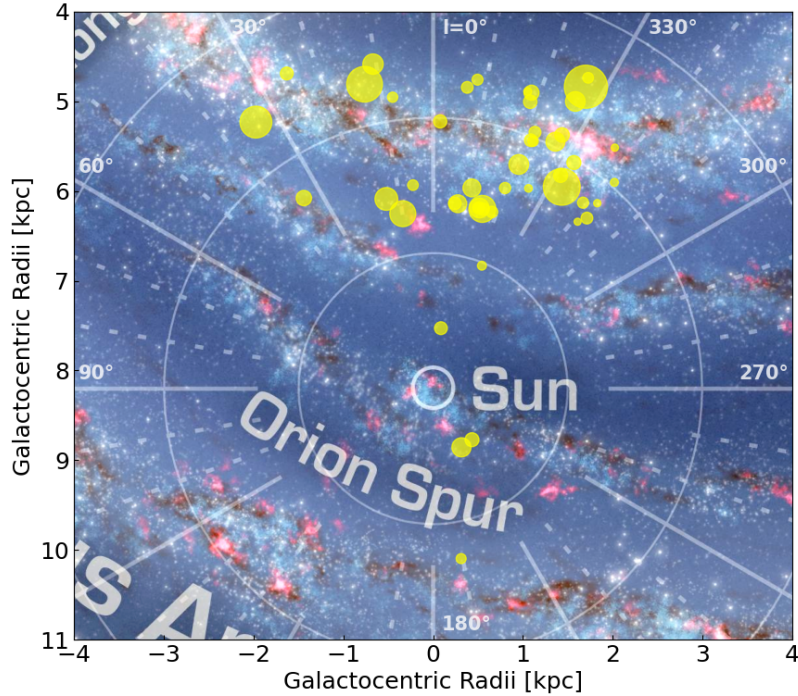


Fig. 1: Locations of the CAFFEINE target regions marked as yellow filled circles in an artist's impression of the Milky Way by R. Hurt (NASA; JPL-Caltech). The area of the circles scales with the solid angle of the field imaged with ArTéMiS at both 350 μm and 450 μm .

Release Content

For each of the 48 fields, we provide two ArTéMiS/SPIRE intensity maps at wavelengths of 350 μm and 450 μm , two ArTéMiS weight maps, and a multi resolution column density map. This results in a total of 240 FITS files. The name, position (in Equatorial coordinates), covered surface area, and median rms noise of the ArTéMiS data at both wavelengths are given in the table below.

Cloud	RA [J2000]	DEC [J2000]	Area [deg ²]	N ₃₅₀ [MJy/sr]	N ₄₅₀ MJy/sr]
MonR2	06:07:47.4	-06:23:11	0.085	299.8	142.2
R5180	06:08:47.2	21:34:30	0.078	242.5	115.3
NGC2264	06:41:03.2	09:30:56	0.093	181.6	99.3
GAL316	14:44:53.1	-59:49:34	0.130	290.5	131.9
I14453	14:48:57.6	-59:26:00	0.051	286.1	148.6
SDC317p7	14:51:11.3	-59:16:32	0.034	277.7	146.1
SDC317p9	14:53:51.3	-59:32:42	0.045	276.3	149.9
RCW87	15:04:24.3	-57:33:36	0.214	211.3	104.9
G322	15:18:34.1	-56:38:09	0.045	333.8	179.2
SDC326	15:43:33.4	-54:02:52	0.345	225.3	119.5
G327	15:52:57.3	-54:36:22	0.101	264.1	141.1
I15541	15:58:06.6	-53:57:55	0.078	404.0	221.0
GAL332	16:15:08.0	-49:49:24	0.098	230.9	114.4

G332	16:16:19.9	-50:52:09	0.185	292.8	153.5
RCW106	16:19:05.9	-51:00:06	0.352	234.9	124.3
G333	16:20:10.0	-49:36:13	0.050	192.9	100.8
G333.2	16:20:55.6	-50:38:09	0.251	427.4	203.4
I16175	16:21:17.5	-50:51:30	0.051	287.5	162.3
G337.1	16:37:44.8	-47:38:53	0.039	211.7	111.3
I16351	16:38:51.8	-47:26:52	0.055	203.7	107.2
I16367	16:40:08.5	-47:09:36	0.085	276.5	133.3
SDC338	16:40:40.5	-46:19:22	0.245	255.9	127.3
G337.9	16:41:16.3	-47:06:27	0.137	258.0	132.5
G339	16:46:04.8	-45:38:26	0.065	243.3	110.8
G340.8	16:51:09.9	-44:44:49	0.156	275.1	137.6
OH341	16:52:37.3	-44:30:52	0.119	203.1	104.0
SDC340	16:54:28.2	-45:14:21	0.124	204.0	107.3
G341.9	16:54:39.5	-43:51:56	0.035	325.2	167.7
RCW116B	17:00:41.9	-40:30:19	0.115	317.4	170.9
I16572	17:00:55.0	-42:23:54	0.090	361.2	169.6
SDC344	17:03:58.4	-42:27:60	0.211	303.7	158.1
SDC345.4	17:04:16.6	-40:44:51	0.067	321.6	175.5
SDC345.0	17:05:23.5	-41:26:51	0.108	203.5	106.1
SDC348	17:19:39.9	-38:57:39	0.165	341.8	165.5
NGC6334N	17:22:33.3	-35:11:27	0.053	170.5	89.0
I17233	17:26:05.6	-36:14:42	0.261	196.2	102.3
NGC6357SE	17:26:09.3	-34:31:55	0.102	245.2	119.8
OH353	17:30:11.4	-34:42:00	0.085	282.3	145.3
G358.5	17:43:32.5	-30:29:23	0.100	269.9	134.6
G005	18:00:30.4	-24:07:17	0.123	216.3	105.6
G008	18:02:33.7	-21:47:54	0.123	279.6	170.5
SDC010	18:09:06.0	-20:12:02	0.346	303.0	157.4
G010	18:09:29.3	-19:42:29	0.153	292.7	142.0
W33	18:14:04.5	-17:42:56	0.471	287.5	131.6
SDC014	18:18:36.4	-16:43:57	0.278	280.5	149.2
W42	18:38:18.5	-06:47:38	0.064	305.6	147.4
G034	18:53:18.3	01:18:47	0.114	206.4	106.3
W48B	18:58:10.5	01:37:10	0.100	293.8	145.3

Release Notes

The detailed steps taken to create the released files are described in Mattern et al. (2024, A&A). In addition to the CAFFEINE ArTéMiS data, our imaging products use additional data from the *Herschel* Space Observatory.

Data Reduction and Calibration

Most of the ArTéMiS data reduction has been done with the APIS software (see <https://www.apex-telescope.org/ns/data-reduction-for-bolometer-arrays/#ArtemisPipeline>).

The data reduction pipeline performs the removal of correlated sky-noise, baseline subtraction, and gridding of the data into a map. Finally, several on-the-fly maps overlapping in a given area are combined to produce pure ArTéMiS maps.

For two of the fields (GAL316 and G337.9), the removal of correlated sky-noise and final map making had to be performed with *Scanamorphos*, a more sophisticated software described in Roussel 2018 and Appendix B of Mattern et al. 2024.

The flux calibration of the ArTéMiS maps has been achieved using skydip observations to measure the zenithal atmospheric opacity at each wavelength, and imaging primary (planets) and secondary calibration sources regularly throughout the observing runs at APEX. The typical uncertainty of the fluxes measured by ArTéMiS is on the order of 20%.

In the further steps of combining the ArTéMiS images with ancillary data from *Herschel*/SPIRE, we employed cross correlation between the ArTéMiS and SPIRE data to further improve the calibration of ArTéMiS specific intensities. The ArTéMiS data were used to correct saturation in some of the *Herschel* (160 to 500 μm) maps. We also used *Planck* data to derive appropriate zero-level offsets for the ArTéMiS/SPIRE intensity maps.

The astrometry of the ArTéMiS observations has been checked every 1-2 hours using well-known reference sources and is estimated to be better than $\sim 3''$.

Data Quality

The mean rms noise level measured in the ArTéMiS/SPIRE intensity maps is about 270 MJy/sr (0.46 Jy/8''-beam) at 350 μm and about 137 MJy/sr (0.37 Jy/10''-beam) at 450 μm , dominated by the ArTéMiS data. However, the noise introduced by the ArTéMiS data varies from field to field and also within a given field, mainly according to the number of independent data points taken around a given position, the weather conditions, and the elevation at which the observations were performed. The histograms of the median rms noise values in each of the ArTéMiS fields is shown at both wavelengths in Fig. 2 below.

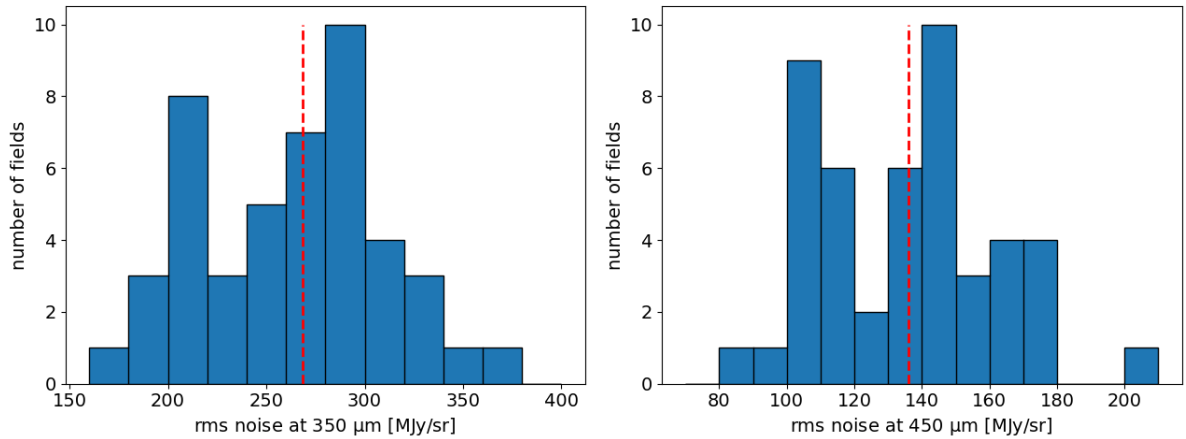


Fig. 2: Histograms of the median rms noise for each of the 48 fields at 350 μm (left) 450 μm (right). The plotted rms noise corresponds to the median standard deviation of the ArTéMiS/SPIRE specific intensities in each field. In each panel, the red dashed line marks the mean value of the distribution.

Known issues

Data Format

File Types

There are five files available for each field. Their file names are structured as:

- “field”_CAFFEINE_coldens_ESO.fits : multi resolution column density map
- “field”_CAFFEINE_350um_ESO.fits : ArTéMiS/SPIRE intensity map at 350 μm
- “field”_CAFFEINE_450um_ESO.fits : ArTéMiS/SPIRE intensity map at 450 μm
- “field”_CAFFEINE_350um_weight_ESO.fits: ArTéMiS weight map at 350 μm
- “field”_CAFFEINE_450um_weight_ESO.fits: ArTéMiS weight map at 450 μm

Acknowledgements

According to the Data Access Policy for ESO data held in the ESO Science Archive Facility, all users are required to acknowledge the source of the data with appropriate citation in their publications.

Please cite Mattern et al. (2024, A&A) and use the following statement in your articles when using these data:

Based on data products from observations made with the Atacama Pathfinder EXperiment (APEX), under ESO programme IDs E-1102.C-0745A-2018 and 106.21MS. APEX is a collaboration between the Max-Planck-Institut für Radioastronomie, the European Southern Observatory, and the Onsala Space Observatory.

Since processed data downloaded from the ESO Archive are assigned Digital Object Identifiers (DOIs), the following statement must also be included in all publications making use of them:

· *Based on data obtained from the ESO Science Archive Facility with DOI: <https://doi.org/10.18727/archive/94>*

Publications making use of data which have been assigned an archive request number (of the form XXXXXX) must include the following statement in a footnote or in the acknowledgement:

· *Based on data obtained from the ESO Science Archive Facility under request number <request_number>.*

Science data products from the ESO archive may be distributed by third parties, and disseminated via other services, according to the terms of the [Creative Commons Attribution 4.0 International license](#). Credit to the ESO provenance of the data must be acknowledged, and the file headers preserved.

References

André, P., Men'shchikov, A., Bontemps, S. et al. 2010, A&A, 518, L102

André, P., Revéret, V., Könyves, V. et al. 2016, A&A, 592, A54

Mattern, M., André, P., Zavagno, A., et al. 2024, A&A, DOI:10.1051/0004-6361/202449908 (arXiv:2405.15713)

Palmeirim, P., André, P., Kirk, J. et al. 2013, A&A, 550, A38

Roy, A., André, P., Palmeirim, P. et al. 2014, A&A, 562, A138

Roussel, H. 2018, arXiv:1803.04264

Schuller, F., André, P., Shimajiri, Y. et al. 2021, A&A, 651, A36